Published in final edited form as:

Clin Cancer Res. 2019 April 15; 25(8): 2601–2609. doi:10.1158/1078-0432.CCR-18-2560.

NQO1-dependent, tumor-selective radiosensitization of non-small cell lung cancers

Edward A. Motea[#1], **Xiumei Huang**[#2], **Naveen Singh**[1], **Jessica Kilgore**[3], **Noelle Williams**[3], **Xian-Jin Xie**[4,§], **David E. Gerber**[5], **Muhammad Shaalan Beg**[5], **Erik A. Bey**[6,*], **David A. Boothman**[1,*]

[1]Department of Biochemistry and Molecular Biology, Simon Cancer Center, Indiana University School of Medicine, Indianapolis, IN 46202 USA

[2]Department of Radiation Oncology, Simon Cancer Center, Indiana University School of Medicine, Indianapolis, IN 46202 USA

[3]Department of Biochemistry, Simmons Comprehensive Cancer Center, University of Texas Southwestern Medical Center, Dallas, TX 75390 USA

[4]Department of Biostatistics, UT Southwestern Medical Center, Dallas, TX 75390 USA

[5]Department of Internal Medicine, Division of Hematology-Oncology, Simmons Comprehensive Cancer Center, University of Texas Southwestern Medical Center, Dallas, TX 75390 USA

[6]Department of Pharmaceutical Sciences, West Virginia University Cancer Institute, Morgantown, WV 26506, USA

[#] These authors contributed equally to this work.

Abstract

Purpose: Development of tumor-specific therapies for the treatment of recalcitrant non-small cell lung cancers (NSCLCs) are urgently needed. Here, we investigated the ability of ß-lapachone (ß-lap, ARQ761 in clinical form) to selectively potentiate the effects of ionizing radiation (IR, 1–3 Gy) in NSCLCs that over-express NAD(P)H:Quinone Oxidoreductase 1 (NQO1).

Experimental Design: The mechanism of lethality of low dose IR in combination with sublethal doses of ß-lap were evaluated in NSCLC lines *in vitro* and validated in subcutaneous and orthotopic xenograph models *in vivo*. Pharmacokinetics and pharmacodynamics (PK/PD) studies comparing single versus co-treatments were performed to validate therapeutic efficacy and mechanism of action.

Results: ß-Lap administration after IR treatment hyperactivated PARP, greatly lowered NAD$^+$/ATP levels, and increased DSB lesions over time *in vitro*. Radiosensitization of orthotopic, as well as subcutaneous, NSCLCs occurred with high apparent cures (>70%), even though 1/8 ß-lap doses reach subcutaneous versus orthotopic tumors. No methemoglobinemia or long-term

[*]Correspondence: erik.bey@hsc.wvu.edu (E.A.B.); dboothm@iu.edu (D.A.B.) (lead).
[§]Present Address: Department of Biostatistics and Computational Biology, University of Iowa, Iowa City, IA

Disclosure of Potential Conflicts of Interest: D.A.B. is an advisor for Systems Oncology, Inc. No potential conflict of interests was disclosed by other authors.

toxicities were noted in any normal tissues, including mouse liver that expresses the highest level of NQO1 (~12 Units) of any normal tissue. PK/PD responses confirm that IR + ß-lap treatments hyperactivate PARP activity, greatly lower NAD^+/ATP levels and dramatically inhibit DSB repair in exposed NQO1+ cancer tissue, while low NQO1 levels and high levels of Catalase in associated normal tissue were protective.

Conclusion: Our data suggest that combination of sublethal doses of ß-lap and IR is a viable approach to selectively treat NQO1-overexpressing NSCLC and warrant a clinical trial using low-dose IR + ß-lapachone against patients with NQO1+ NSCLCs.

STATEMENT OF TRANSLATIONAL RELEVANCE

Lung cancer remains the leading cause of cancer-related death in men and women in North America. Patients diagnosed with non-small cell lung cancer (NSCLC) have few effective treatment options, which cause undesirable side-effects due to lack of tumor selectivity when used at higher doses. There is an urgent need for personalized strategies to selectively target cancer while sparing normal tissue. This study delineates the mechanistic basis for tumor-selective potentiation of ionizing radiation (IR) in combination with β-lapachone (β-lap, ARQ761 in clinical form), an NQO1-bioactivatable agent that induces lethal DNA damage in recalcitrant NSCLCs (~90% overexpress NQO1 as a biomarker). Non-toxic doses of β-lap can be combined after treatment with IR to selectively and synergistically kill NSCLCs with no apparent normal tissue toxicity *in vivo*. Our findings warrant a clinical trial to combine sublethal doses of IR + ß-lap against patients with NQO1(+) NSCLCs for precision-guided medicine.

Keywords

lung cancer; ionizing radiation; NQO1; beta-lapachone; reactive oxygen species

INTRODUCTION

We previously demonstrated that ß-lap was a unique substrate for NAD(P)H:Quinone Oxidoreductase 1 (NQO1) (E.C.1.6.5.2) (1–10), wherein the enzyme performs a futile two-electron oxidoreduction of the compound using NAD(P)H to generate an unstable hydroquinone form of ß-lap (7,10,11). Unique to this quinone, its hydroquinone form is highly unstable and spontaneously undergoes two oxidoreductive back-reactions to its original drug form (1,3–7,10–15). NQO1 thereby constantly undergoes a futile redox cycle using NAD(P)H and creating two moles of superoxide in the two-step back-reaction (6,7). A tremendous pool of NAD(P)+ forms (4,6–9,12,16,17), along with very high levels of superoxide, which are rapidly converted to hydrogen peroxide (H_2O_2). High doses of H_2O_2 eventually damages the DNA of NQO1+ cancer cells (15,18,19). The reaction can also cause a strong lethal effect in adjacent $NQO1^{Low}$ cancer cells in the same tumor via an H_2O_2-dependent bystander effect mediated by low catalase levels in these cancers (15). AP (apurinic, apyrimidinic, or abasic) sites, DNA single strand breaks (SSBs) and DNA double strand breaks (DSBs) form in NQO1+ cancer cells exposed to ß-lap via a strong PARP1 hyperactivation (6,7,12,16), which then degrades the heightened NAD^+ levels resulting from NQO1-dependent redox cycling of this unique quinone (3,4,7,10,15,20). This process is mediated by H_2O_2-induced release of calcium from endoplasmic reticulum (ER) stores

(12,16). Delineating the mechanism of action of ß-lap has revealed exciting synergistic combinations, for example, using glutamate synthase inhibitors (BEPTES, CB089) (18), DNA base excision repair inhibitors (methoxyamine and XRCC1 depletion) (19), as well as PARP inhibitors (10). Analyses of numerous NQO1-expressing breast, prostate, lung, pancreatic and head and neck cancer cells shows that ß-lapachone (a prototypic NQO1 bioactivatable drug) kills cancer cells by an NQO1-dependent ischemia-reperfusion mechanism independent of oncogenic driver or passenger statuses, regardless of p53 or cell cycle status, and independent of over-expressed anti-apoptotic mechanisms (e.g., Bcl2, Bax loss) that may drive resistance (10).

We previously exploited ß-lapachone as a radiosensitizer of cancer cells *in vitro*, initially without knowing the mechanism by which synergistic killing with IR occurred (21,22). After determining the mechanism of action of ß-lap, we then used NQO1 over-expressing human prostate or head and neck cancer xenograft mouse models to show how the compound radiosensitized human cancers *in vivo* (11,23). Our data showed that synergy could be accomplished using IR + ß-lap via creation of normal, rapidly repaired DNA lesions that simultaneously hyperactive PARP1, where IR or drug alone did not separately meet the DNA damage required. Here, we demonstrate that ß-lap suppresses IR-induced DSB repair and we illustrate the efficacy of IR + ß-lap treatments against non-small cell lung cancers (NSCLCs) that commonly have significantly elevated levels of NQO1, but concomitantly low Catalase (Cat) levels (10). We also tested the hypotheses that massive PARP1 hyperactivation reactions after IR + ß-lap led to dramatic accompanying NAD^+/ATP losses that ultimately inhibit DSB repair processes (initiated by IR exposure) and may lead to NQO1-dependent NAD^+-Keresis cell death (14) responses specific for NQO1+ NSCLC tumors. No methemoglobinemia or toxicities to normal tissues were found in IR + ß-lap-exposed mice. Data presented in this study warrants a clinical trial using low-dose radiotherapy with the clinically available NQO1 bioactivatable drug (ARQ761) against NSCLCs containing wild-type NQO1 as a biomarker for personalized medicine.

MATERIALS AND METHODS

Reagents and chemicals.

β-Lapachone (ß-lap) was synthesized and purified by us (6). Dicoumarol (DIC), hydrogen peroxide (H_2O_2), Hoechst 33342, bovine serum albumin, and cytochrome *c* were purchased from Sigma-Aldrich (St. Louis, MO). HPβCD (>98% purity) was purchased from Cyclodextrin Technologies Development, Inc. (High Springs, FL) and β-lap-HPβCD was prepared as described (24).

NQO1 enzyme assays.

NQO1 enzyme activities from cancer cells or tumor or normal tissues were measured as dicoumarol-inhibited units either with or without cytochrome C (1,25).

Cell lines and tissue culture.

Human nonsmall cell lung cancer (NSCLC) cells were generated by the UTSW-MD Anderson SPORE in lung cancer (26) or other cells were purchased (Lewis lung carcinoma,

A549) from the American Tissue Culture Collection (Manassas, VA). Cells were grown as described (10) and routinely screened free of mycoplasma.

Cell culture irradiations and colony forming ability assays.

All cell culture irradiations were performed using a Mark 1 irradiator with a ^{137}Cesium source delivering a dose rate of 3.49 Gy/minute (JL Shepherd & Associates, San Fernando, CA). Varying doses of β-lap dissolved in DMSO (± Dicoumarol) were added immediately after irradiation and incubated with the drug for two hours in a humidified incubator (37 °C, 5% CO_2). After two-hour treatment, media was replaced with fresh complete media and allowed to grow for several doubling periods. Colony forming ability assays were performed using 500–15,000 cells per 100 mm plates as described (21,22). Colonies of >100 healthy normal-appearing cells were counted and normalized to vehicle-treated control cells.

Antibodies.

Antibodies used for immunofluorescence and Western blotting, included: NQO1 (A180), PARP1 (SC-8007, Santa Cruz, La Jolla, CA), ß-actin (C4, Santa Cruz), PAR (Trevigen, Gaithersburg, MD), 53BP1 (Santa Cruz), γ-H2AX (JBW301, Millipore, Temecula, CA), phosphorylated ATM (p-ATM-s1981), total-ATM (t-ATM) and α-tubulin (Santa Cruz).

Western blot assessments.

Westerns were performed using ECL chemiluminescent detection and density analyses using NIH ImageJ with intensity normalization (6,7,10,25).

DSB detection and repair.

Cells were imaged by immunofluorescence using Leica DM5500 fluorescent microscopy for a marker of DSB formation. The number of 53BP1 foci in a given cell nucleus was quantified and graphed as percent (%) nuclei with ≥10 53BP1 foci/nucleus (6,7,25). Alternatively, for assessments *in vivo*, γ-H2AX levels were screened and quantified by Western blotting (10).

Tumor irradiations and antitumor activity assays.

Luciferase-labeled tumors (LLC-luc or NSCLC-luc) were generated by injecting 5×10^6 tumor cells into the subcutaneous space on the backs, or into tail veins to generate orthotopic xenografts, of female athymic nude mice or NSG mice weighing 18–20 grams obtained from the UT Southwestern institutional breeding core. In general, survival and tumor volume data were graphed from two separate studies, each with 10 combined mice/group. Bioluminescence imaging (BLI), antitumor activity, and survival studies using subcutaneous (300 mm^3) or orthotopic NSCLC (A549) xenograft-bearing athymic nude or NSG mice were performed. Subcutaneous Lewis lung carcinoma (LLC) tumors (200 mm^3) were raised in a same manner. Four weeks after implantation, mice were treated with or without various doses of IR (Gy), using specific collimators for delivery only to the lung or subcutaneous tumor flank areas every other day for five treatments. Immediately following IR treatments, mice were then exposed iv with or without HPβCD or sub-lethal doses of β-lap-HPβCD by tail vein injection (9). Animals were irradiated using an X-RAD 320 small animal irradiator

(Precision X-Ray, North Branford, CT). For combination IR + β-lap-HPβCD treatments, β-lap-HPβCD was administered within 30 min post-IR. Tumor volumes were either directly measured using calipers (for subcutaneous models) and/or using Bioluminescence (BLI)-based tumor volume estimates for orthotopic models (7,10). Long-term survival and target validation assays were performed with log-rank tests for survival (7,9,10). All animal studies were carried out under a University of Texas at Southwestern Medical Center Institutional Animal Care and Use Committee (IACUC) approved protocol and in accordance with the guidelines for ethical conduct in the care and use of animals in research.

Biomarker and pharmacokinetic analyses (PK/PD).

Pharmacokinetics (PK) of β-lap levels in blood, tumor and normal tissues were assessed by LC-MS/MS analyses following extraction of plasma, tumor or normal tissue homogenates with acetonitrile (7,9,10,27). An unpaired t-test (GraphPad QuickCalcs, San Diego, CA) was used to evaluate significant differences in β-lap concentrations after different treatments. Pharmacodynamic (PD) parameters of PAR formation and γH2AX in normal tissue and tumors were simultaneously performed using pooled samples from three animals per time point (7,10,27). Please refer to the Supplementary Information for a more detailed description of the ATP, NAD^+/NADH quantification in tumor lysates at indicated treatment conditions.

Statistical Analysis.

Data (means, ± standard deviations) were graphed and ANOVA used to compare groups. Two-tailed Student's t-tests for independent measures with Holm-Sidak correction for multiple comparisons, if >1 comparisons, were performed. Minimum replicate size for any experiment was n=3. Alpha was set to 0.05. Curve fitting and calculation of LD_{50} values, ANOVA, and two-tailed Student t-tests for statistical significance were performed in GraphPad Prism 6.0. Images were representative of experiments or stainings repeated three times. *p<0.05; **p<0.01; ***p<0.001; and ****p<0.0001.

Synergy Calculations.

Synergy interactions between two drugs were evaluated as previously described (10) using two methods: **1**) Direct comparisons made between the effect of combined treatments and the effect of individual drugs in each experiment; and **2**) Formal synergy effects evaluations used a strict method proposed by Chou and Talalay (28) and Lee et al., (29) where pooled, multiple dose-responses for each of the treatments were required.

RESULTS

ß-Lapachone (ß-lap) exerts NQO1-dependent radiosensitization of NSCLC cells.

A549 NSCLC cells express high levels of NQO1 typical of most NSCLC tumors, with relatively low expression of catalase, so they are a good representative cell line model to use (10). A549 cells are hypersensitive to ß-lap, where inhibiting NQO1 activity with dicoumarol greatly suppressed lethality (Fig. 1A). A striking dose-response with NQO1+ cells is noted, where 3 μM ß-lap (2 h) results in cell stress with minimal lethality (~80% survival) and 4 μM (2 h) causes significant cell death (>LD_{50}) as previously demonstrated to

be through programmed necrosis (10). Irradiation of A549 cells with lower doses of IR (1–3 Gy) and then exposing cells immediately thereafter with sublethal doses of ß-lap (1–3 μM, Fig. 1A) resulted in significant dose-response increases in lethality (Fig. 1B). Radiosensitization was also noted when cells were exposed to higher IR doses (>3 Gy) in combination with lower concentrations (<LD_{50}) of ß-lap (1–3 μM) (Fig. 1B). Administration of dicoumarol (DIC), a well-utilized NQO1 inhibitor (10), prevented lethality of irradiated (2–7 Gy) A549 cells co-treated with ß-lap (3 μM). Similarly, H1650 NSCLC cells exposed to IR (2 Gy) and then treated immediately with various concentrations of ß-lap (1–5 μM) for 2 h post-irradiation, exhibited significant synergistic responses compared to 2 Gy IR dose alone, or to various low doses of ß-lap alone (Fig. 1C). Radiosensitization of IR + ß-lap was prevented by inhibiting NQO1 via co-administration of 50 μM dicoumarol immediately following IR (Fig. 1C), suggesting NQO1-dependent lethal effects. H1650 cells express ~100 units of NQO1, which is sufficient to induce a synergistic effect. As previously reported (21,22), adding low doses of ß-lap before IR treatment could lead to no discernable synergistic responses in A549 or H1650 NSCLC cells.

IR-induced DSB repair is inhibited by ß-lapachone.—Exposure of NQO1+ A549 cells with ß-lap alone causes specific DNA lesions, including AP sites and DNA single strand breaks (18,19) that result in the hyperactivation of PARP activity, noted by a significant accumulation of poly(ADP-ribose)-PARP (PAR-PARP) post-translational protein modification (Fig. 2A); note that PAR-PARP may represent an inactive form of the enzyme (6,10). PARP hyperactivation is strongly induced within 5–10 mins of ß-lap exposure. Thereafter, PAR-PARP1 levels were dramatically decreased due to loss of NAD^+ levels (PARP substrate to produce PAR) (6,7,10) within 20–30 mins during exposure and simultaneous removal of PAR moieties from the PARP1 protein by Poly(ADP-ribosyl) glycohydrolase (PARG) (Fig. 2A). Interestingly, the activation of ATM (formation of pS1981-ATM) and formation of γ-H2AX were significantly delayed in cells exposed to ß-lap and were not significantly apparent until after PARP hyperactivation was exhausted. These data suggest that PARP activity binds and protects AP sites and SSBs, but once PARP activity is exhausted cells attempt to either replicate over the damage, or the damage becomes hypersensitive to the stress caused by high levels of ß-lap-induced H_2O_2 (7,10), and DSBs are formed. ATM is then activated, which phosphorylates H2AX (γ-H2AX) (Fig. 2A). While major reductions of NAD^+/ATP levels are observed in these cells, there appears to be significant levels of nuclear dATP to drive ATM activation and γ-H2AX formation over the 2 h time-period (Figs. 2A, B) (17).

We hypothesized that exposure of NQO1+ NSCLC cells to IR + ß-lap resulted in the inhibition of DSB repair, due to significant losses of NAD^+/ATP resulting from PARP hyperactivation and conversion of DNA single strand lesions caused by IR + ß-lap to elevated DSBs. A549 cells were exposed to IR (2 Gy) and then treated with a sublethal dose of ß-lap, shown to result in significant radiosensitization (Fig. 1B), to monitor DSB repair over time using 53BP1 foci formation/nucleus assessments (Figs. 2C–D). Data were then graphed showing DSB formation (% nucleus with ≥10 53BP1 foci formation/nucleus) over time (Fig. 2D, Supplemental Fig. 1). ß-Lap treatment of IR-exposed A549 cells resulted in substantial formation of DSBs per cell nucleus within the two-hour treatment (Figs. 2C–D)

followed by a significant inhibition of DSB repair compared to IR-treated or ß-lap-exposed cells alone 4 h post-treatment (Supplemental Fig. 1A–B). Approximately less than 10% of cells repaired any significant level of DSBs over the 120 mins post-irradiation time when ß-lap was administered (Figs. 2C, D). In contrast, the significant formation of DSBs noted after IR alone were rapidly repaired within 120 mins (Figs. 2C, D). Exposure of A549 cells to 3 μM ß-lap only caused a low level of delayed DSB formation at 120 mins, which does not lead to a lethal effect with this dose of drug (Fig. 1B). The effects of ß-lap on IR-induced DSB repair were reversed by NQO1 inhibition by dicoumarol.

Radiosensitization of subcutaneous NSCLC by ß-lap.—We then established subcutaneous xenografts (~400 mm^3) using A549 cells in female athymic nude mice and treated these mice every other day for 5 injections with: (**a**) HPßCD vehicle alone (iv); (**b**) IR (2 Gy) alone, only around the xenograft with collimator shielding; (**c**) ß-lap (20 mg/kg, iv) alone; or (**d**) IR (2 Gy) + 20 mg/kg HPßCD-ß-lap, administered iv immediately after IR treatment. Treatment of subcutaneous A549 NSCLC xenografts with ß-lap (20 mg/kg, iv) alone is a very ineffective therapeutic regimen, where some growth suppression occurs, but regrowth occurs in a rapid manner (Figs. 3A–C) (7). Likewise, IR (2 Gy) alone, given every other day for 5 doses had no significant antitumor or long-term survival effects compared to vehicle (HPßCD) alone (Figs. 3A–C). In contrast, treatment with IR (2 Gy) + ß-lap (20 mg/kg, iv) exhibited synergistic antitumor effects, with tumor regression from days 5–16 compared to vehicle or IR alone and a significant overall apparent cure rate of ~80% of exposed mice bearing xenografts. No methemoglobinemia nor normal tissue toxicities were noted at 90 days post-treatment and apparently cured mice lived to >300 days post-treatment. At euthanasia at 350 days, no notable tumor was found within the legs of these IR + ß-lap-treated mice. Pharmacokinetic analyses of mice bearing subcutaneous *vs* orthotopic A549 xenografts grown at the same time in female athymic nude mice revealed that subcutaneous xenografts accumulated 8-fold less drug (ß-lap) than in orthotopic A549 xenografts (Fig. 3D, Supplemental Fig. 2). Levels of ß-lap in A549 tumor, plasma, lung and other tissue over time (mins) are represented in Supplemental Fig. 3, where significant levels of ß-lap were found in lung tissue and relatively lower levels found in subcutaneous A549 tumor tissue. The higher levels of the drug in lung tissue, suggested that we examine orthotopic NSCLC antitumor and survival effects. Moreover, A549 NSCLC subcutaneous tumors (200–400 mm^3) show significant synergistic responses to 8 Gy (Supplemental Fig. 4A) or 10 Gy (Supplemental Fig. 4B) + ß-lap (30 mg/kg, iv) given every other day for 5 injections, with no significant methemoglobinemia or weight loss (Supplemental Fig. 5).

Radiosensitization of subcutaneous Lewis lung carcinoma (LLC) xenografts that express lower levels of NQO1.—LLC cells express significantly less NQO1 activity (~50 units/mg tissue) compared to A549 NSCLC cells, which express >350 units/mg tissue (10). LLC levels of NQO1 are still ~5- to 100-fold above normal tissue expression of NQO1, with liver tissue NQO1 levels being the highest in these mice at ~10.3 ±0.2 Units/mg tissue. We examined the ability of ß-lap to radiosensitize low NQO1-expressing LLC xenografts (Fig. 4), exposing 300 mm^3 xenografts with varying doses of IR (0, 2, 4 8 Gy) alone, varying doses of ß-lap (10 or 20 mg/kg) alone or with 2 Gy IR + 10 or 20 mg/kg ß-lap given every other day for 5 treatments total (Fig. 4). Minimal antitumor

effects were noted with 20 mg/kg ß-lap or IR (2 Gy) alone, or with combination IR (2 Gy) + 10 mg/kg ß-lap. However, exposure of LLC xenograft-bearing athymic mice to IR (2 Gy) + 20 mg/kg ß-lap iv immediately after IR treatment caused a significant increase in survival, with ~50% apparent cures at 40 days (Fig. 4). These mice exhibited no weight loss or methemolobinemia responses (trouble breathing, lethargy) and remained alive with no apparent LLC tumor levels out to 200 days. In addition, necropsy at 200 days showed no toxicities to normal tissue nor tumor tissues.

ß-Lapachone radiosensitizes orthotopic NSCLC tumors with low drug levels.

We then examine the ability of ß-lap to radiosensitize orthotopic A549 NSCLCs. A549-luc derived cells were used to develop orthotopic A549 NSCLC xenografts in athymic nude mice (Fig. 5A), where animal CT scanning of orthotopic tumors were visualized and tumor tissue confirmed by immunohistochemical analyses (Fig. 5A). Mice bearing significant A549 tumor volumes (Fig. 5A) were treated every other day, for five total doses, with IR (2 Gy) using collimator-guided irradiations with or without 10, 20 or 30 mg/kg HPßCD-ß-lap (iv). Mice were also treated with ß-lap alone at the same doses and frequency. Antitumor effects were noted with 20 and 30 mg/kg ß-lap, as well as IR (2 Gy X 5) alone, but significant antitumor effects were noted at 40 days post-treatment with IR + 10, 20 or 30 mg/kg ß-lap (Fig. 5B). ß-lap alone caused significant increases in survival in a dose-dependent manner, with 10 mg/kg affording little antitumor (Fig. 5B) or overall survival advantage. In contrast, 20 and 30 mg/kg ß-lap alone caused dramatic increases in antitumor effects (Fig. 5B) and survival advantages, with 35 and 50 day increases in survival at LD_{50} levels (Fig. 5C). IR alone caused significant increases in antitumor effects (Fig. 5B) and survival (Fig. 5C), but no overall apparent cures in A549-bearing mice. In contrast, a significance enhancement of antitumor effects (Fig. 5B) and overall survival (Fig. 5C), where 50% (for 10 mg/kg ß-lap) and 60% (for 20 and 30 mg/kg ß-lap) apparent cures were noted at 300 days; synergy in terms of overall survival between IR + ß-lap versus IR or ß-lap alone was noted as per Chou and Talalay calculations.(28) No overall weight loss or methemoglobinemia were noted with any IR alone, ß-lap alone or IR + ß-lap treatments (Fig. 5D).

Biomarker analyses reveals DSB repair inhibition from PARP hyperactivation *in vivo* in A549 orthotopic xenografts.—As treated above, athymic nude mice bearing A549 orthotopic xenografts were exposed to IR (2 Gy) alone, ß-lap (20 mg/kg, iv) alone or to 2 Gy + ß-lap (20 mg/kg iv). Mice (3/group) were then euthanized over time for assessment of PAR-PARP levels (Fig. 6A), DSBs via γ-H2AX (Fig. 6B), as well as NAD^+ and ATP levels (Figs. 6C, D). While ß-lap alone caused significant increases in PAR-PARP levels (Fig. 6A), with late forming DSBs (Fig. 6B) and decreases in NAD^+ and ATP (Fig. 6C, D), changes in these same levels in A549 xenografts after IR + ß-lap were dramatically greater (Figs. 6A–D). We noted that after IR + ß-lap, PAR-PARP formation occurred early within 5–30 mins then decreased by 120 min, while DSB formation increased late between 30–120 mins. These data are consistent with effects of IR + ß-lap noted *in vitro* in A549 culture cells (Figs. 2A–B). In contrast, exposure of tumors with IR (2 Gy) alone resulted in no increases in PAR-PARP formation, DSBs (i.e., γ-H2AX (at 30 or 60 mins), or in NAD^+

or ATP level losses (Figs. 6A–D). The kinetics of PAR-PARP formation, and NAD^+ and ATP losses are shown in Supplemental Figs. 6A–C.

DISCUSSION

NQO1 bioctivatable drugs, such as ß-lapachone, are competent tumor-selective agents for selective use against cancers that express elevated levels of NQO1, such as found in non-small cell lung cancers (NSCLC) (10). Here, we demonstrated that the drug is an efficacious radiosensitizing agent if added immediately after IR treatment in NQO1+ NSCLC. Interestingly, the drug does not work if pretreated prior to IR exposure. It is possible that radiation therapy first transiently primes the tumors to facilitate the accumulation and delivery of β-lap-HPβCD by modifying the local tumor microenvironment (i.e. vascular bursting) as previously reported with other chemical agents (30–32). It is also conceivable that IR treatment could induce NQO1 protein expression, and thus increased enzymatic activity, to generate more reactive oxygen species with the addition of ß-lap (33). However, we have previously reported that the lethal effect of ß-lap (LD_{50} values) remains relatively constant at ≥100 Units of NQO1 activity in multiple cell lines and cancer types (23). These possibilities require further optimization and investigation. Mechanistically, we envision that the generation of potentially clustered ROS-induced nucleobase damage, DNA single strand breaks and extensive apyrimidinic/apurinic (AP) sites by both agents at low doses leads to the hyperactivation of PARP, with dramatic losses of NAD^+ and ATP. The contribution of DSBs by IR treatment, with minimally significant levels induced by ß-lap (Figs. 2C–D, Supplemental Fig. 1, Fig. 6B), immediately causes lethal DNA lesions with the combination treatments that then may not be repaired efficiently due to the dramatic losses of NAD^+ and ATP, which are the energetic currency utilized by various DNA damage response and repair factors for efficient function (Supplemental Fig. 7). Increased PAR-PARP formation with concomitant lowered levels of NAD^+ and ATP are consistent with PARP hyperactivation. We monitored increased DSB formation through assessment of 53BP1 (Figs. 2C, D, Supplemental Fig. 1) and γ-H2AX (Fig. 6B) when IR + ß-lap treatments were given *in vitro* and *in vivo,* respectively. All of the radiosensitizing effects of ß-lap in NSCLC (Fig. 1C), prostate (11) or head and neck (23) cancers were prevented by dicoumarol (DIC), and were not seen in NQO1- cancer cells. The net effect of IR + ß-lap is efficacious radiosensitization of NQO1+ cancer cells, with minimal effects on methemoglobinemia or normal tissue toxicities. The efficacy of IR + ß-lap in preclinical models using NSCLCs (Figs. 3–6) against both subcutaneous as well as orthotopic xenografts, warrants a Phase I clinical trial. ARQ761 is currently in two phase I clinical trials as a monotherapy against solid cancers, as well as used in combination with gemcitabine and Abraxane against pancreatic cancers. Therefore, the phase I maximum tolerable dose is already known and will be reported soon.

A major impact of the IR + ß-lap combination therapy is the specificity of the combination against specific NQO1 over-expressing cancers. Recently, we reported high levels of NQO1 expression in a majority of NSCLC (10), pancreatic (18,19), prostate (11), breast (15) and head and neck (23) cancers. Interestingly, we also reported that most NSCLC and pancreatic cancers that over-expressed NQO1 concomitantly under-express catalase (10) that neutralizes H_2O_2, thus contributing to the efficacy of IR + ß-lap by elevating and prolonging H_2O_2 half-lives and increasing tumor-selective DNA damage needed for PARP

hyperactivation and NAD+ degradation. The exhaustion of PARP activity through hyperactivation most likely further elevates DSB break formation over time. Thus, we anticipate that IR + ß-lap treatments would be an extremely efficacious tumor-selective therapy against a wide range of solid cancers. The therapy would allow significant lowering of IR and ß-lap doses compared to using either agent alone. The data presented in this study reveals a number of novel biomarkers that could be used to examine the efficacy of ß-lap (ARQ761 in clinical form) when specifically combined with IR therapies against NSCLC. Collectively, our *in vitro* and *in vivo* data may provide the impetus needed to (1) translate our findings in the clinic; (2) examine other types of tumors that overexpress NQO1 as a biomarker for selective and synergistic lethality using our combination therapy; and (3) investigate other novel NQO1-bioactivatable drugs in conjunction with ionizing radiation.

Supplementary Material

Refer to Web version on PubMed Central for supplementary material.

ACKNOWLEDGEMENTS

We are grateful to the UT Southwestern Simmons Comprehensive Cancer Center support grant (5P30CA142543) for use of cores (biostatistics, bioinformatics, preclinical pharmacology (PK)) and Jaideep Chaudhary for technical assistance. This work was supported by NIH/NCI R01CA224493-01 to DAB.

REFERENCES

1. Pink JJ, Planchon SM, Tagliarino C, Varnes ME, Siegel D, Boothman DA. NAD(P)H:Quinone oxidoreductase activity is the principal determinant of beta-lapachone cytotoxicity. The Journal of biological chemistry 2000;275:5416–24 [PubMed: 10681517]
2. Planchon SM, Pink JJ, Tagliarino C, Bornmann WG, Varnes ME, Boothman DA. beta-Lapachone-induced apoptosis in human prostate cancer cells: involvement of NQO1/xip3. Experimental cell research 2001;267:95–106 [PubMed: 11412042]
3. Reinicke KE, Bey EA, Bentle MS, Pink JJ, Ingalls ST, Hoppel CL, et al. Development of beta-lapachone prodrugs for therapy against human cancer cells with elevated NAD(P)H:quinone oxidoreductase 1 levels. Clinical cancer research : an official journal of the American Association for Cancer Research 2005;11:3055–64 [PubMed: 15837761]
4. Bentle MS, Reinicke KE, Bey EA, Spitz DR, Boothman DA. Calcium-dependent modulation of poly(ADP-ribose) polymerase-1 alters cellular metabolism and DNA repair. The Journal of biological chemistry 2006;281:33684–96 [PubMed: 16920718]
5. Bentle MS, Reinicke KE, Dong Y, Bey EA, Boothman DA. Nonhomologous end joining is essential for cellular resistance to the novel antitumor agent, beta-lapachone. Cancer research 2007;67:6936–45 [PubMed: 17638905]
6. Bey EA, Bentle MS, Reinicke KE, Dong Y, Yang CR, Girard L, et al. An NQO1- and PARP-1-mediated cell death pathway induced in non-small-cell lung cancer cells by beta-lapachone. Proc Natl Acad Sci U S A 2007;104:11832–7 [PubMed: 17609380]
7. Huang X, Dong Y, Bey EA, Kilgore JA, Bair JS, Li LS, et al. An NQO1 substrate with potent antitumor activity that selectively kills by PARP1-induced programmed necrosis. Cancer research 2012;72:3038–47 [PubMed: 22532167]
8. Blanco E, Bey EA, Dong Y, Weinberg BD, Sutton DM, Boothman DA, et al. Beta-lapachone-containing PEG-PLA polymer micelles as novel nanotherapeutics against NQO1-overexpressing tumor cells. Journal of controlled release : official journal of the Controlled Release Society 2007;122:365–74 [PubMed: 17574288]

9. Blanco E, Bey EA, Khemtong C, Yang SG, Setti-Guthi J, Chen H, et al. Beta-lapachone micellar nanotherapeutics for non-small cell lung cancer therapy. Cancer research 2010;70:3896–904 [PubMed: 20460521]

10. Huang X, Motea EA, Moore ZR, Yao J, Dong Y, Chakrabarti G, et al. Leveraging an NQO1 Bioactivatable Drug for Tumor-Selective Use of Poly(ADP-ribose) Polymerase Inhibitors. Cancer Cell 2016;30:940–52 [PubMed: 27960087]

11. Dong Y, Bey EA, Li LS, Kabbani W, Yan J, Xie XJ, et al. Prostate cancer radiosensitization through poly(ADP-Ribose) polymerase-1 hyperactivation. Cancer research 2010;70:8088–96 [PubMed: 20940411]

12. Tagliarino C, Pink JJ, Dubyak GR, Nieminen AL, Boothman DA. Calcium is a key signaling molecule in beta-lapachone-mediated cell death. The Journal of biological chemistry 2001;276:19150–9 [PubMed: 11279125]

13. Dong Y, Chin SF, Blanco E, Bey EA, Kabbani W, Xie XJ, et al. Intratumoral delivery of beta-lapachone via polymer implants for prostate cancer therapy. Clinical cancer research : an official journal of the American Association for Cancer Research 2009;15:131–9 [PubMed: 19118040]

14. Moore Z, Chakrabarti G, Luo X, Ali A, Hu Z, Fattah FJ, et al. NAMPT inhibition sensitizes pancreatic adenocarcinoma cells to tumor-selective, PAR-independent metabolic catastrophe and cell death induced by beta-lapachone. Cell death & disease 2015;6:e1599 [PubMed: 25590809]

15. Cao L, Li LS, Spruell C, Xiao L, Chakrabarti G, Bey EA, et al. Tumor-selective, futile redox cycle-induced bystander effects elicited by NQO1 bioactivatable radiosensitizing drugs in triple-negative breast cancers. Antioxid Redox Signal 2014;21:237–50 [PubMed: 24512128]

16. Tagliarino C, Pink JJ, Reinicke KE, Simmers SM, Wuerzberger-Davis SM, Boothman DA. Mu-calpain activation in beta-lapachone-mediated apoptosis. Cancer biology & therapy 2003;2:141–52 [PubMed: 12750552]

17. Wuerzberger SM, Pink JJ, Planchon SM, Byers KL, Bornmann WG, Boothman DA. Induction of apoptosis in MCF-7:WS8 breast cancer cells by beta-lapachone. Cancer research 1998;58:1876–85 [PubMed: 9581828]

18. Chakrabarti G, Moore ZR, Luo X, Ilcheva M, Ali A, Padanad M, et al. Targeting glutamine metabolism sensitizes pancreatic cancer to PARP-driven metabolic catastrophe induced by ß-lapachone. Cancer Metabolism 2015;3:12 [PubMed: 26462257]

19. Chakrabarti G, Silvers MA, Ilcheva M, Liu Y, Moore ZR, Luo X, et al. Tumor-selective use of DNA base excision repair inhibition in pancreatic cancer using the NQO1 bioactivatable drug, beta-lapachone. Sci Rep 2015;5:17066 [PubMed: 26602448]

20. Pink JJ, Wuerzberger-Davis S, Tagliarino C, Planchon SM, Yang X, Froelich CJ, et al. Activation of a cysteine protease in MCF-7 and T47D breast cancer cells during beta-lapachone-mediated apoptosis. Experimental cell research 2000;255:144–55 [PubMed: 10694431]

21. Boothman DA, Greer S, Pardee AB. Potentiation of halogenated pyrimidine radiosensitizers in human carcinoma cells by beta-lapachone (3,4-dihydro-2,2-dimethyl-2H-naphtho[1,2-b]pyran-5,6-dione), a novel DNA repair inhibitor. Cancer research 1987;47:5361–6 [PubMed: 3652040]

22. Boothman DA, Trask DK, Pardee AB. Inhibition of potentially lethal DNA damage repair in human tumor cells by beta-lapachone, an activator of topoisomerase I. Cancer research 1989;49:605–12 [PubMed: 2535961]

23. Li LS, Reddy S, Lin ZH, Liu S, Park H, Chun SG, et al. NQO1-Mediated Tumor-Selective Lethality and Radiosensitization for Head and Neck Cancer. Molecular cancer therapeutics 2016;15:1757–67 [PubMed: 27196777]

24. Nasongkla N, Wiedmann AF, Bruening A, Beman M, Ray D, Bornmann WG, et al. Enhancement of solubility and bioavailability of beta-lapachone using cyclodextrin inclusion complexes. Pharm Res 2003;20:1626–33 [PubMed: 14620518]

25. Li LS, Bey EA, Dong Y, Meng J, Patra B, Yan J, et al. Modulating endogenous NQO1 levels identifies key regulatory mechanisms of action of beta-lapachone for pancreatic cancer therapy. Clinical cancer research : an official journal of the American Association for Cancer Research 2011;17:275–85 [PubMed: 21224367]

26. Skoulidis F, Byers LA, Diao L, Papadimitrakopoulou VA, Tong P, Izzo J, et al. Co-occurring genomic alterations define major subsets of KRAS-mutant lung adenocarcinoma with distinct

biology, immune profiles, and therapeutic vulnerabilities. Cancer Discov 2015;5:860–77 [PubMed: 26069186]

27. Ma X, Huang X, Moore Z, Huang G, Kilgore JA, Wang Y, et al. Esterase-activatable beta-lapachone prodrug micelles for NQO1-targeted lung cancer therapy. Journal of controlled release : official journal of the Controlled Release Society 2015;200:201–11 [PubMed: 25542645]
28. Chou TC, Talalay P. Quantitative analysis of dose-effect relationships: the combined effects of multiple drugs or enzyme inhibitors. Adv Enzyme Regul 1984;22:27–55 [PubMed: 6382953]
29. Lee JM, Ledermann JA, Kohn EC. PARP Inhibitors for BRCA1/2 mutation-associated and BRCA-like malignancies. Ann Oncol 2014;25:32–40 [PubMed: 24225019]
30. Miller JA, Kotecha R, Ahluwalia MS, Mohammadi AM, Suh JH, Barnett GH, et al. The impact of tumor biology on survival and response to radiation therapy among patients with non-small cell lung cancer brain metastases. Pract Radiat Oncol 2017;7:e263–e73 [PubMed: 28254368]
31. Bentzen SM, Harari PM, Bernier J. Exploitable mechanisms for combining drugs with radiation: concepts, achievements and future directions. Nat Clin Pract Oncol 2007;4:172–80 [PubMed: 17327857]
32. Miller SM, Wang AZ. Nanomedicine in chemoradiation. Ther Deliv 2013;4:239–50 [PubMed: 23343162]
33. Park HJ, Ahn KJ, Ahn SD, Choi E, Lee SW, Williams B, et al. Susceptibility of cancer cells to beta-lapachone is enhanced by ionizing radiation. Int J Radiat Oncol Biol Phys 2005;61:212–9 [PubMed: 15629614]

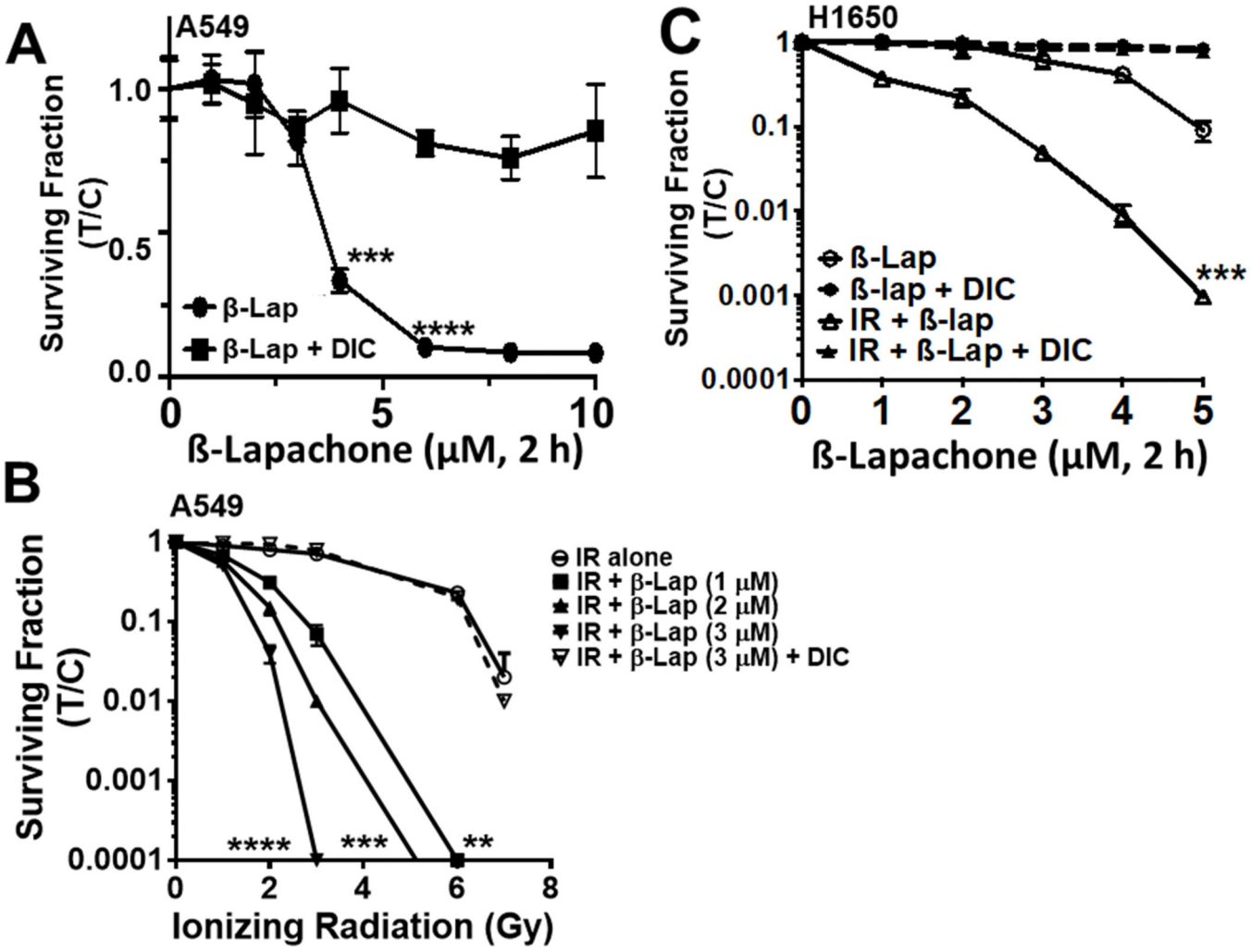

Figure 1. Radiosensitization of human NSCLC cells by ß-lapachone.

A. Log-phase A549 NSCLC cells were exposed or not to varying doses of ß-lap for 2 h, with or without 50 µM dicoumarol (DIC), a fairly specific inhibitor of NQO1. **B.** Log-phase A549 cells were treated with or without various doses of IR (1–7 Gy) and then immediately exposed or not to sublethal (<LD_{50}) doses of ß-lap (1–3 µM, 2h). DIC prevented radiosensitization of A549 cells exposed to 2 Gy + 3 µM ß-lap (highest sublethal dose used). **C.** Log-phase H1650 NSCLC cells were exposed or not to IR (2 Gy) and then immediately treated or not with varying doses of ß-lap (µM, 2h), with or without 50 µM dicoumarol (DIC).

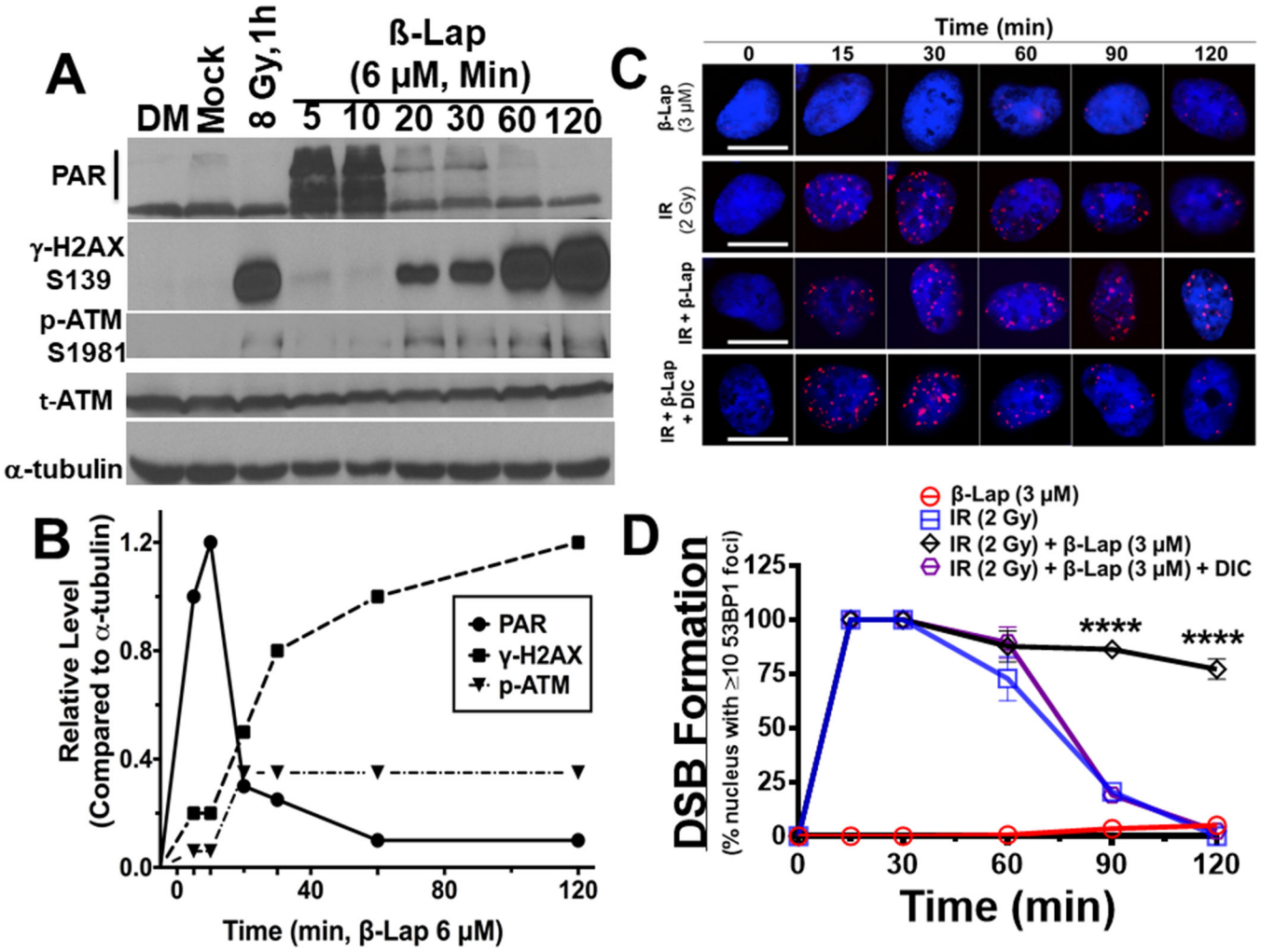

Figure 2. ß-Lap inhibits DNA double strand break repair.

A. Log-phase A549 NSCLC cells were treated with or without ß-lap (6 μM) and cell extracts prepared at various times during treatment to detect PAR-PARP formation, γ-H2AX (pS139), pS1981 ATM, total ATM (t-ATM) and α-tubulin steady state levels by Western blot. A549 cells were also exposed or not to IR (8 Gy) and analyzed 1 h later. Mock, non-irradiated cells. DM, media alone. **B.** Graphical representation of data shown in Fig. 2A. **C.** Representative images of A549 cells exposed or not to IR (2 Gy) alone, ß-lap (3 μM, 2h) alone, the combination [IR (2 Gy) + ß-lap (3 μM, 2h), or the combination with DIC (50 μM, NQO1 inhibitor) and assessed for DSB breaks over time (0–120 min) using 53BP1 as the surrogate marker (in red). Cells were also stained for nuclear DNA using DAPI (in blue). Scale bar = 10 μm. **D.** Graphical representation of data presented in Fig. 2C. ****p<0.0001.

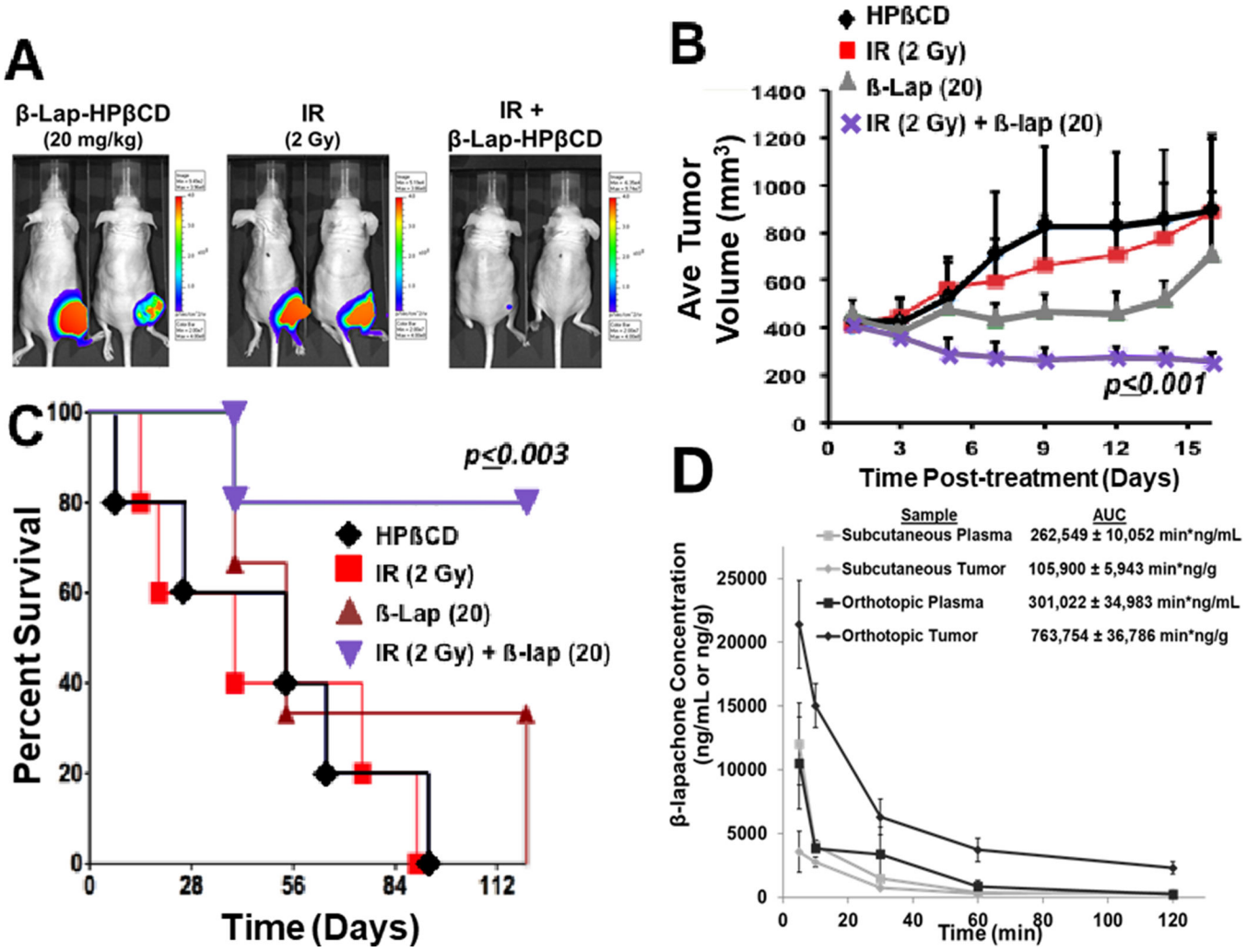

Figure 3. ß-Lap radiosensitizes subcutaneous A549-luc xenografts in athymic nude mice.

A. Subcutaneous A549-luc xenografts (400 mm^3) were generated in athymic nude mice and then treated with or without IR (2 Gy) then immediately with or without ß-lap (20 mg/kg) for 5 treatments every other day. Representative antitumor responses (at day 20 post-treatment) are demonstrated for ß-lap alone, IR alone, and the IR + ß-lap combination. **B.** Antitumor responses (tumor volumes, mm^3) over time are shown for the treatments described in Figs. 3A. **C.** Overall survival of animals treated as described in Figs. 3A. **D.** PK values for plasma and subcutaneous versus orthotopic A549-luc tumors in athymic nude mice. Note the significantly high levels of ß-lap in orthotopic vs subcutaneous A549 tumor tissue, whereas plasma levels were identical in both sets of mice. See Supplemental Fig. 2 for additional PK data.

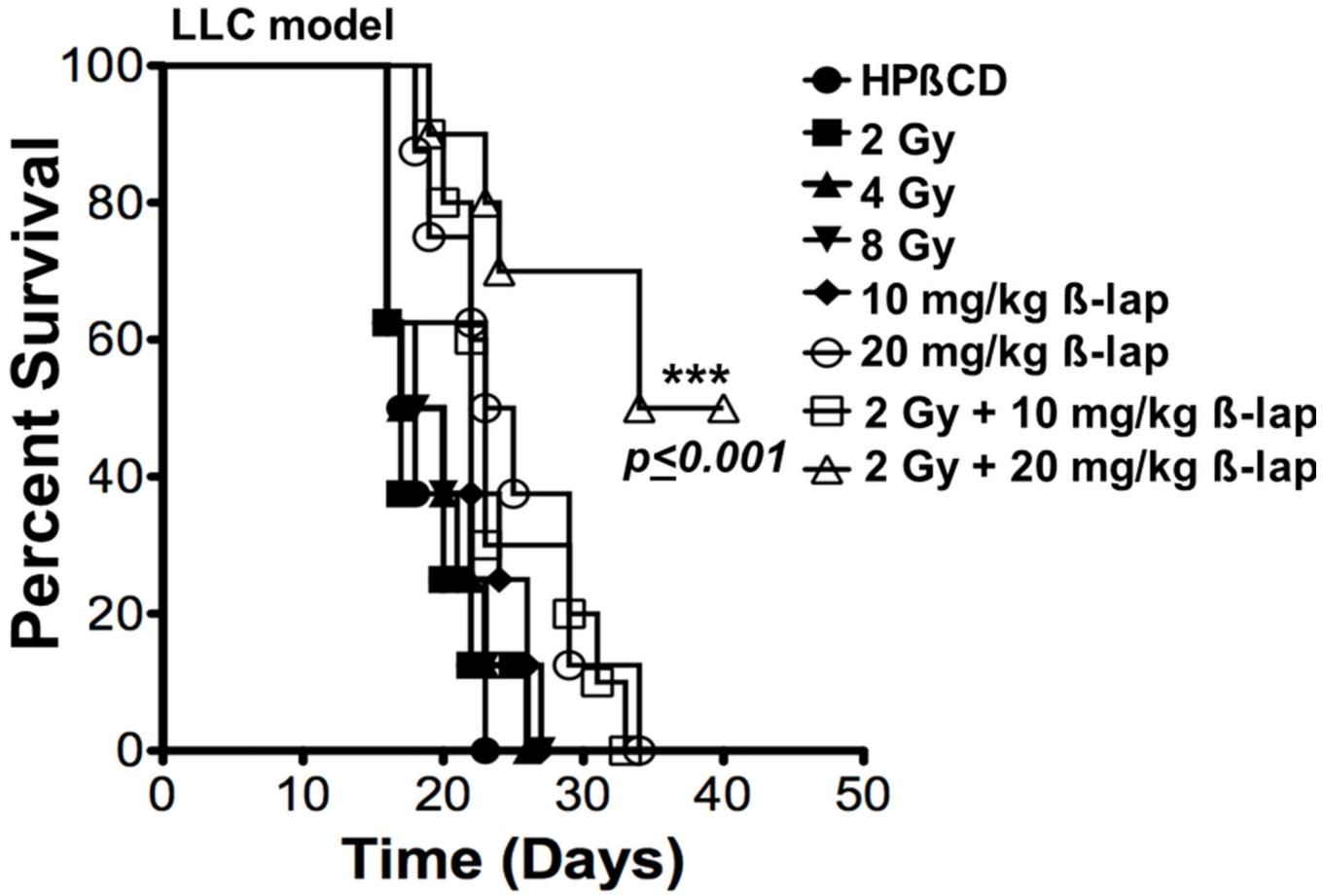

Figure 4. ß-Lap radiosensitizes Lewis lung carcinoma (LLC) xenografts in athymic nude mice.

LLC subcutaneous xenografts (300 mm^3) were generated in athymic nude mice and treated with HPßCD alone, as well as 2, 4, and 8 Gy alone. Mice were also treated with ß-lap (10 or 20 mg/kg, iv) alone. Finally, mice were also treated with 2 Gy + 10 or 20 mg/kg ß-lap. Mice were treated every other day with 2 Gy and then immediately with ß-lap (10 or 20 mg/kg, iv). Survival of the treated LLC-bearing mice were then monitored over time (to 40 days). N=10 mice/group. ***, $p<0.001$.

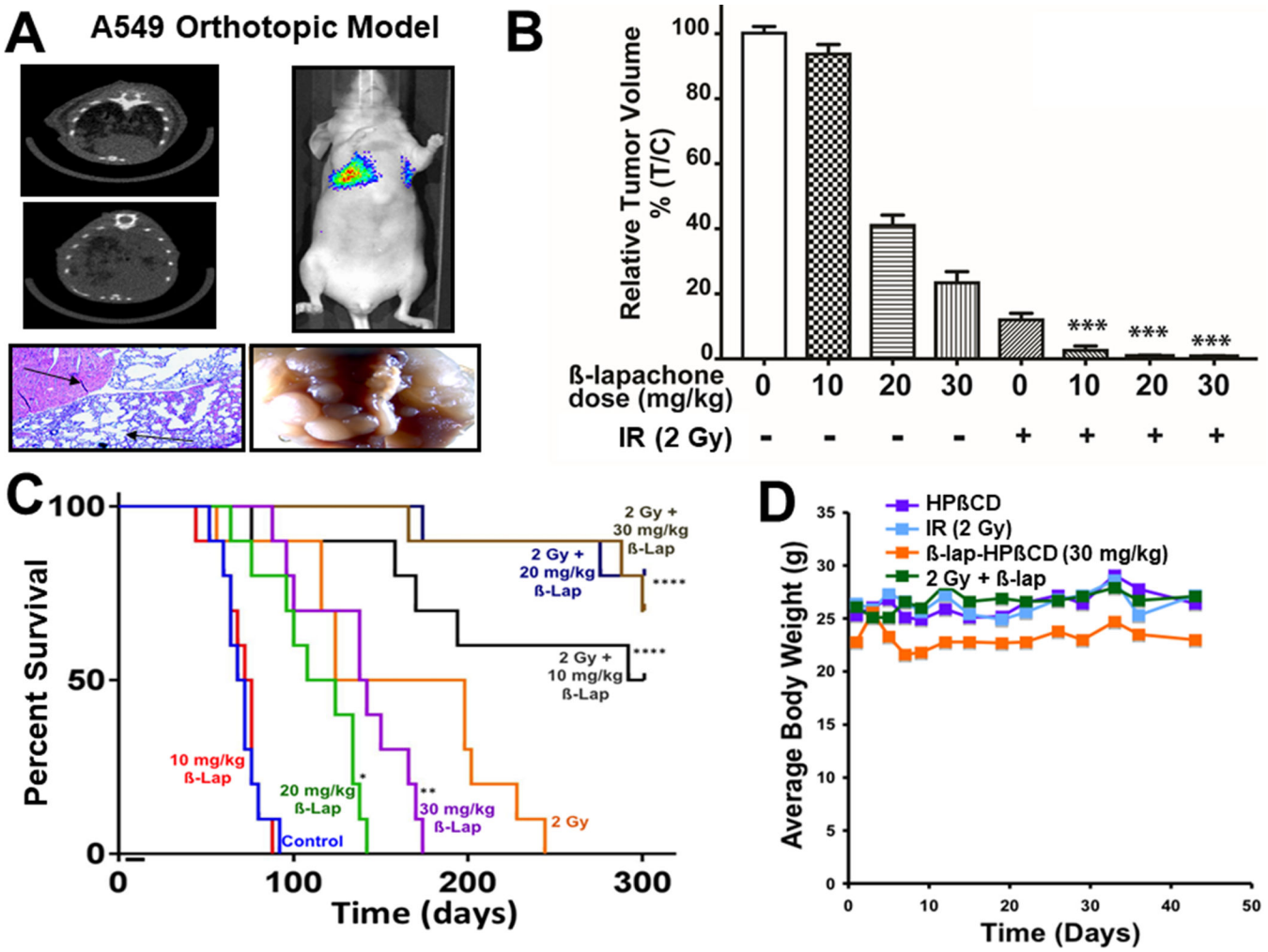

Figure 5. ß-Lap radiosensitizes orthotopic A549-luc xenografts in athymic nude mice.

A. Imaging of A549-luc mice and IHC analyses of tumor vs associated normal tissue. Top left, CT scan of control and A549 tumors. Top right, BLI analyses of a mouse bearing A549-luc. Bottom left, IHC of tumor (red, arrow) and associated normal tissue (blue). Bottom right, extracted A549 tumor. **B.** Tumor volumes (%T/C) at 20 days post-treatment before and after ß-lap alone (10, 20, or 30 mg/kg, iv) without or with IR (2 Gy) pretreatment. Mice were treated every other day for 5 treatments and BLI measurements were performed at 10, 20 30 and 40 days. Shown are results representative of all measurements at 20 days. N=10 animals/group, ***, $p<0.001$. **C.** Overall survival of mice in Fig. 5B *, $p<0.5$; **, $p<0.01$; $p<0.001$; ***, $p<0.0001$; $p<0.00001$. **D.** Weight changes monitored for mice treated with or without 2 Gy, ß-lap (30 mg/kg, iv) and IR (2 Gy) + ß-lap (30 mg/kg, iv) every other day for 5 treatments.

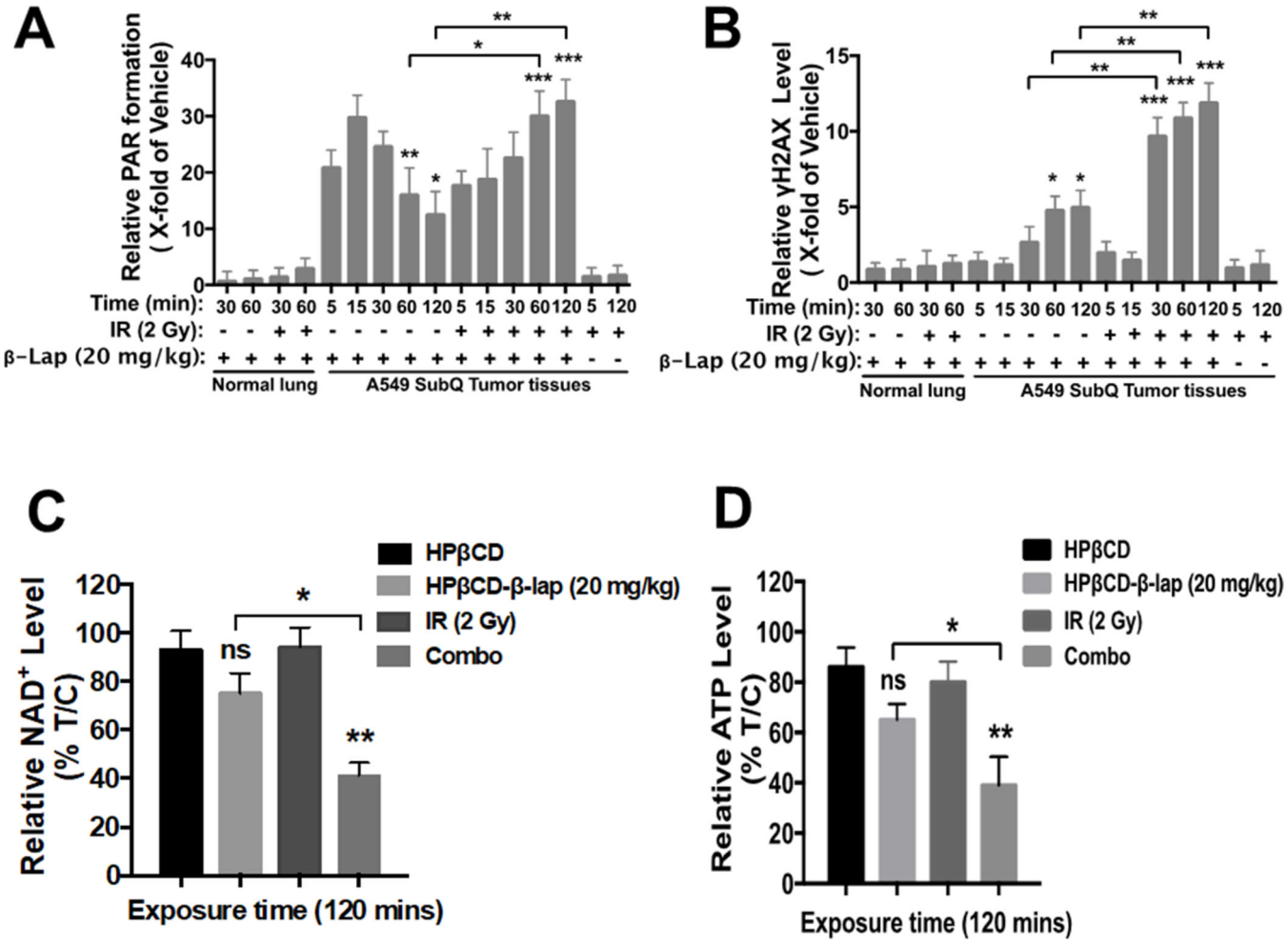

Figure 6. Biomarker analyses after IR + ß-lap indicate increased PAR formation, increased DNA double strand breaks (γ−H2AX) with concomitant decreases in NAD^+/ATP.

A-D. A549-luc-bearing mice (3/group) were treated as described in Fig. 5B, then sacrificed at various times post-treatment. Pooled extracts were then assessed for (**A**) PAR-PARP formation; (**B**) γ−H2AX; as well as (**C**) NAD^+ and (**D**) ATP levels. *, p<0.05; **, p<0.01; ***, p<0.001; and ****, p<0.0001. See Supplemental Fig. 6 for additional data.